Sensitivity analysis of THOR-50M thorax injury criteria to test variations in a vehicle driver configuration

Daiki Furukawa, Andre Eggers

Abstract This study quantifies the influence of parameter variations on THOR-50M thorax injury criteria in a production vehicle environment. Frontal sled simulations were performed using a THOR-50M simulation model in a driver seat environment with 50 km/h MPDB pulse. Upper and lower thorax stiffness, initial dummy postures, shoulder-belt routing, load limiter force and driver airbag pressure were selected as variation parameters. The parameter ranges were set to those expected in physical testing, based on the Euro NCAP procedure or expert recommendations. R_{max}, *PC Score* and *TIC_NFR* were evaluated. A Design of Experiments (DOE) study of 200 simulations was performed. All criteria were more sensitive to upper thorax stiffness than to others. The variation in R_{max} ranged from 29 mm to 46 mm and, for the load case in this study, this may lead to a change of up to two levels in the rating score (Euro NCAP colour band scheme). These findings highlight the importance of minimising the influence of THOR-50M upper thorax variation in physical testing for the performance evaluation of safety systems and assessment programs. While injury criteria should remain sensitive to restraint system properties, there is a need for investigation of robust criteria that are not too sensitive to variations of the measurement equipment (dummy).

Keywords Frontal crash, THOR-50M, Injury criteria, Testing variability, Sensitivity analysis.

I. INTRODUCTION

To evaluate occupant protection performance in frontal crashes, Euro NCAP introduced the MPDB (Mobile Progressive Deformable Barrier) test in 2020 [1]. In this test, the THOR-50M (Test Device for Human Occupant Restraint 50M) dummy is positioned in the driver seat. In comparison with the widely used Hybrid III dummy, THOR-50M has been reported to provide improved biofidelity and is equipped with a larger set of measurement channels, including 3D displacement sensors in the thorax and abdomen. During its development, repeated sled tests demonstrated good repeatability and reproducibility, with coefficients of variation (CV) below 10% for most injury outcomes [2]. Additionally, Euro NCAP has defined a qualification procedure for the THOR-50M to ensure consistent performance in crash tests [3]. Despite these efforts, previous studies have reported variability in injury outcomes, particularly chest deflection, in repeated frontal sled tests conducted in both generic and vehicle environments [4-5]. These studies have highlighted its potential influence on assessment results. Furthermore, if the influence of testing variability is comparable to or greater than the performance improvement achieved by advanced restraint systems, it may obscure the benefits of those systems and affect their proper evaluation. As a result, testing variability may complicate not only fair and consistent assessment but also the development and implementation of improved occupant protection systems. To address these challenges, previous research has studied the effects of dummy structural components (e.g. ribs and flex joints) on chest deflection through simulations and component level tests [6-8]. Additionally, sensitivity studies have investigated how variations in seat-belt properties and routing affect thorax injury outcomes [9]. However, in vehicle crash tests, these variations occur simultaneously, and their combined influence is difficult to isolate. A previous study that systematically investigated the influence of variation parameters that could occur in vehicle tests using simulations showed that the upper thorax stiffness of the THOR-50M is a highly sensitive parameter for thorax injury criteria [10]. However, this study was conducted in a simplified generic environment, which may not fully represent the characteristics of seats and restraint systems in the production vehicle. Therefore, the aim of this study is to investigate the influence of variability expected in physical crash testing on occupant kinematics and

D. Furukawa (e-mail: daiki_furukawa@mail.toyota.co.jp) is an assistant manager in Advanced Product Development Div. at Toyota Motor Corporation, Japan. A. Eggers, PhD, is a researcher at Federal Highway and Transport Research Institute (BASt), Germany.

Injury outcomes using a CAE model of a production vehicle environment. With this model a simulation-based investigation was conducted to quantify the individual effects of each parameter.

II. METHODS

A parameter study was conducted that consisted of frontal sled simulations with a simulation model of THOR-50M in a production vehicle environment. Repeated sled tests were carried out within this study in one baseline condition to validate the sled simulation model.

Frontal sled testing

Three repeated sled tests were conducted with a small SUV driver environment (Fig. 1). THOR-50M with H-III leg was positioned according to the Euro NCAP procedure [1], and all tests were conducted using the same dummy. A 50 km/h MPDB pulse (Fig. 2) from in-house full vehicle crash test was used as a sled acceleration pulse. The occupant load criterion (OLC) [11] of sled pulse ranged from 24.5 g to 25.0 g. The sled test setup consisted of a Body in White, a driver seat, a retractor with load limiter and pretensioner, a driver airbag, a knee airbag and an instrument panel, all representative of a modern production vehicle configuration. Detailed specifications of these components are confidential and are therefore not provided in this paper. For the knee airbag, the fabric of the airbag was taken out of the case, but it was not inflated in its initial state. The deployment timing (time-to-fire) of the knee airbag was set 5 ms later than that of the other restraint systems because of this modified initial configuration. For the initial dummy positioning, the target position was defined according to the Euro NCAP procedure [1]. The H-point was kept within ±1 mm (X- and Z- directions) of the target position across tests, and the pelvic angle was maintained within 33 ± 0.1 degrees in the Y direction. The restraint systems were obtained from the same production batch, and the time-to-fire was kept identical for all tests.

Fig. 1. Side view of sled testing.

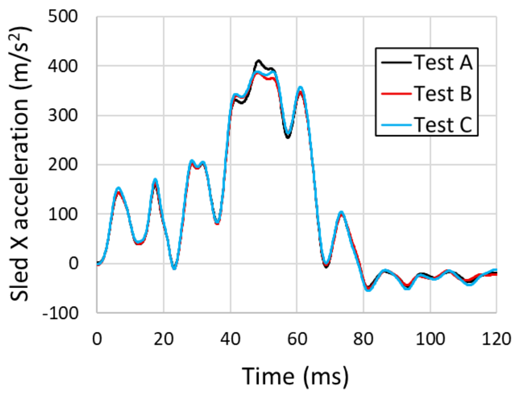

Fig. 2. Sled acceleration pulse.

Frontal Sled Simulation

Frontal sled simulations were performed using identical vehicle package and sled acceleration pulse with a THOR-50M Euro NCAP borderline model (V1.8, Humanetics Innovative Solutions) [12]. Ansys LS-DYNA R11.2 solver [13] was used for these simulations. The simulation model, including a retractor with load limiter and pretensioner, a driver airbag and a knee airbag, was validated against the results of repeated sled tests. Based on the test results, the deployment timing of the knee airbag was set 3 ms later than that of the other restraint system in this simulation model. As a baseline model, dummy initial posture and seat-belt routing were set as close as possible to match conditions measured in physical sled tests. For belt routing, the relative vertical distance between lower neck bolt and upper edge of the shoulder-belt was used as the quantitative parameter (Appendix Fig. A1). This parameter was selected because chest deflection was a key outcome in this study, and it was important to match the relative position of the shoulder-belt to the chest deflection measurement location in the physical tests and the simulation. Since the location of the chest deflection sensor cannot be measured directly in the physical tests, the lower neck bolt was used as a practical reference point because its coordinates can be measured in the physical tests, and it is located close to the upper chest measurement region.

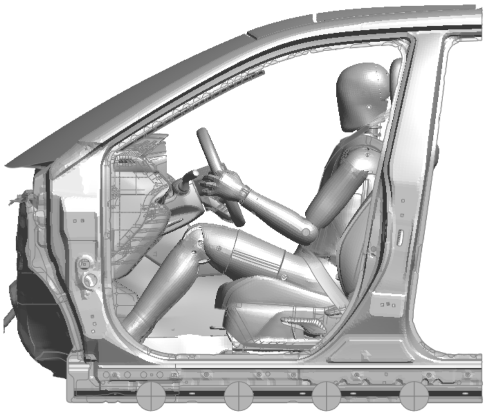

Fig. 3. Side view of sled simulation model.

Variation Parameters in Sled Simulation

Parameters of the dummy parts, test boundary conditions and restraint system were selected as those variation parameters considered to be highly influential. For the dummy parameters, upper and lower thorax stiffness were selected because they are related to certification characteristics of the THOR-50M and can be adjusted using the “borderline model” function of the THOR-50M dummy model. In this study, the term “thorax stiffness” refers to the thorax response characteristics represented by the borderline model, rather than a directly measured physical stiffness parameter. In the borderline model, the user specifies target certification (impactor) responses for the upper and lower thorax, and the corresponding internal model parameters are determined accordingly. In this study, the upper thorax stiffness was defined based on the chest resultant deflection in the upper thorax certification responses, whereas the lower thorax characteristic was defined based on the chest X-axis deflection in the lower thorax certification responses. Five levels were selected for both the upper and lower thorax characteristics using the corresponding certification responses, such that the resulting responses were expected to be within the range of Euro NCAP upper and lower thorax certification corridors [14]. A total of 25 possible thorax stiffness combinations were considered. As test boundary conditions, shoulder-belt routing and initial dummy posture (H-point location) were considered (Fig. 4). The initial shoulder-belt routing was adjusted, while the buckle position and the D-ring location were kept unchanged. A variation range of ±10 mm was assumed for this parameter as a practical estimate of the possible variation in belt routing that may occur in physical testing, based on expert experience. Forward and rearward postures were defined by adjusting H-point location in the X-direction to fall within accepted tolerances of the Euro NCAP MPDB procedure. Considering the seat-pan angle, the H-point height (Z-direction) position was adjusted according to the X-direction H-point position, and no changes were made to the seat position. The pelvic angle (Y axis) was also adjusted within the Euro NCAP tolerances to maintain the contact between torso and seat back. Neck/T1 tilt angle and heel position were set to match the baseline posture as closely as possible. The shoulder-belt routing for all adjusted postures was determined such that the vertical distance between the lower neck bolt and the upper edge of the shoulder-belt was identical to that of the baseline posture. Load limiter force and driver airbag pressure were selected for the restraint system parameters. A load limiter force variation of ±8% from the baseline and a driver airbag pressure variation of ±10% from the baseline were assumed. These variations were generated by scaling the magnitude of the simulation input curves for the load limiter force and driver airbag pressure (inflator property), i.e. the physical quantity on the vertical axis of each input curve. The variation ranges for the restraint system were selected as representative engineering ranges that may occur in physical testing, based on expert experience and practical knowledge of production level variation.

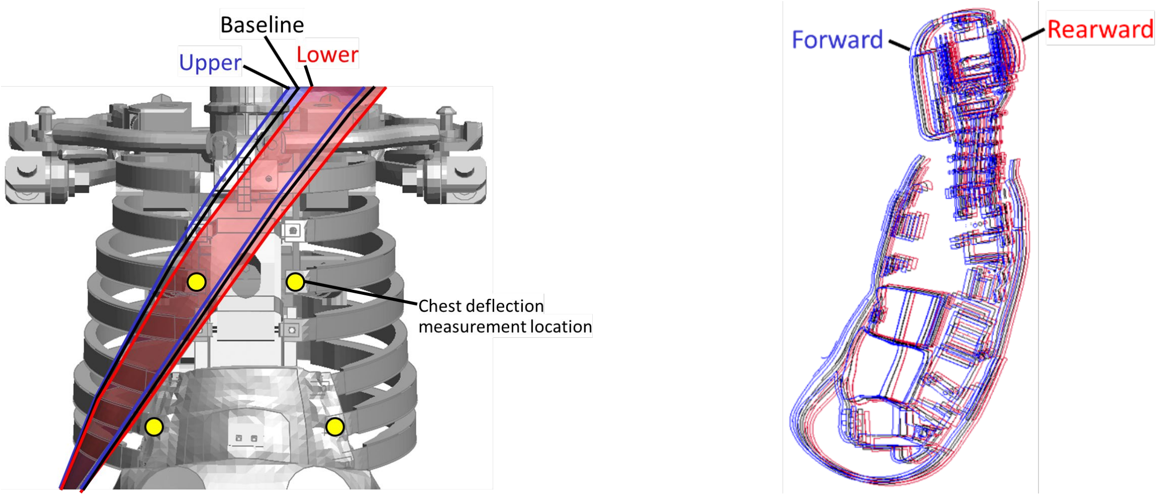

(a) Shoulder-belt routing. (b) Dummy initial posture.

Fig. 4. Variation parameters of test boundary conditions.

Sled Simulation Matrix (DOE)

A total of 200 simulations were performed, and the simulation matrix for the design of experiments (DOE) was generated using a Latin Hypercube sampling design in LS-OPT [15]. Table I shows the summary of the variation parameters and range. Within the parameter ranges, shoulder-belt routing was set at three discrete levels, whereas the other parameters were set at five discrete levels. The baseline simulation used for model validation was defined by the baseline values of all parameters listed in Table I.

TABLE I
VARIATION PARAMETERS

Parameter		Unit	Minimum	Baseline	Maximum
Dummy	Upper Thorax stiffness	mm	47.5	51.1	54.7
	Lower Thorax stiffness	mm	-52.4	-49	-45.6
Boundary condition	Initial dummy posture (H-point)	mm	-13	0	13
	Belt routing	mm	63	73	83
Restraint system	Load limiter force	%	92	100	108
	Driver airbag pressure (inflator property)	%	90	100	110

Injury criteria

R_{max}, *PC Score* and thoracic injury criterion (*TIC_NFR*) were evaluated [16-19]. R_{max} is currently being assessed by Euro NCAP [19]. *PC Score* and *TIC_NFR* were calculated using multi-point chest deflection measurements. Table II summarises the injury criteria and the injury risk functions used in this study. The calculation of injury probabilities was conducted, assuming an occupant age of 45 years.

TABLE II
THORAX INJURY CRITERIA AND INJURY RISK FUNCTIONS FOR THE THOR-50M (45 YEARS OLD)

Criteria	Calculation	Injury Risk Function	Injury Level	Reference
R_{max}	$\max(UL_{max}, UR_{max}, LL_{max}, LR_{max})$	$1 - e^{-\left(\frac{R_{max}}{e^{(4.7276-0.0166a)}}\right)^{2.977}}$	AIS 3+	[16]
PC Score	$0.486\left(\frac{up_{tot}}{17.439}\right) + 0.492\left(\frac{low_{tot}}{14.735}\right) + 0.496\left(\frac{up_{dif}}{9.672}\right) + 0.526\left(\frac{low_{dif}}{12.384}\right)$	$1 - e^{-\left(\frac{PC\ Score}{e^{(2.8677-0.0181a)}}\right)^{3.311}}$	AIS 3+	[17]
TIC_NFR	$Rmax + 1.66\ up_{dif}$	$1 - e^{-\left(\frac{TIC\_NFR}{e^{(5.2675-0.0135a)}}\right)^{\frac{1}{0.09325+0.00475a}}}$	NFR 3+	[18-19]

a: Age
$up_{tot} = |UL|_{max} + |UR|_{max}$, $up_{dif} = |UL - UR|_{max}$, $low_{tot} = |LL|_{max} + |LR|_{max}$, $low_{dif} = |LL - LR|_{max}$

III. RESULTS

Model Validation

A comparison of the responses for the major channels, showing the results of the baseline sled simulation and the three repeated sled tests, are presented in Fig. 5, Fig. 6 and Fig. 7. The baseline simulation corresponds to the case defined by the baseline parameter values listed in Table I, including the input parameters of the borderline model. The ISO scores [20] calculated from the simulation results and from each repeated sled test are shown in Table III, and Table IV summarises thorax injury outcomes from simulation and sled tests. The channels listed in Table III correspond to the Euro NCAP Virtual Testing procedure [20], and the resultant accelerations for the occupant are also calculated as reference. For chest deflection, the scores based on the resultant chest deflection are shown. The ISO score exceeded the 0.5 threshold specified in the Euro NCAP procedure for all channels except head Y-axis acceleration and chest Y- and Z-axis accelerations. Under the test conditions considered in this study, these accelerations were small compared with the X-axis acceleration. The small Y-axis response is likely because only an X-axis acceleration pulse was applied in both the sled tests and the simulation. The small chest Z-axis acceleration is likely due to the initial orientation of the chest Z-axis accelerometer being close to horizontal and the limited forward excursion of the upper body. Although these scores were below the Euro NCAP threshold, the influence of these accelerations on occupant kinematics was considered minor compared with that of X-axis accelerations in this study. The ISO scores for chest deflection were calculated using the resultant chest deflections. These scores ranged from 0.58 to 0.74 (average) and exceeded the Euro NCAP threshold. At the upper right position, where the maximum chest deflection is typically observed, differences were observed in the rise time of the pulse (approximately 5 ms), the timing of the peak (15–17 ms), and the peak chest deflection value (8–10 mm). Similar tendencies were observed at the other measurement points as well. For the pelvis acceleration shown in Fig. 5(c), the simulation generally agreed with the repeated test results, however, the simulation showed a higher peak around 26 ms than the experimental data. This is likely due to the knee airbag interaction, which results in a higher reaction force during knee contact in the simulation than in the physical tests. Although this suggests room for further refinement of the vehicle model, its influence on the main conclusions of this study was considered limited. The repeated sled tests showed response trends in the major channels that were generally similar to the simulation results, although some variation was observed in peak timing and peak magnitude. A summary of the repeatability of these baseline sled tests is provided in Appendix Table B1. Table IV shows that the injury outcomes predicted by the baseline simulation were lower than those measured in the repeated tests. Despite these differences, the model was considered suitable for evaluating relative tendencies caused by the variation parameters with respect to the baseline condition, which was the primary objective of this study.

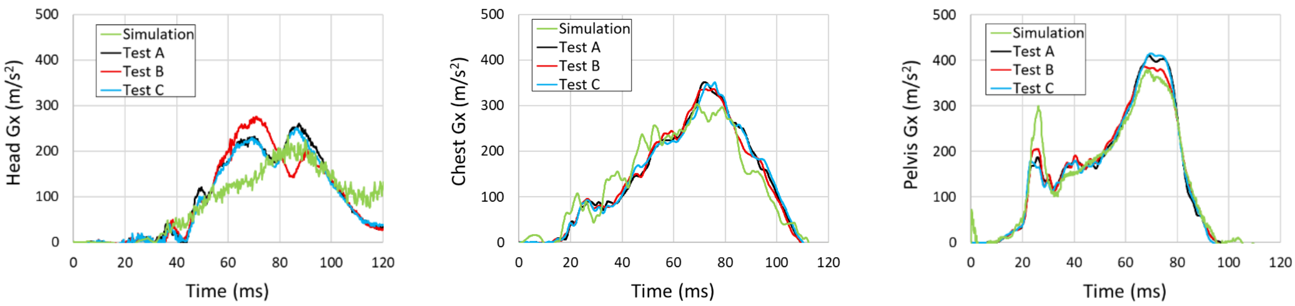

(a) Head X acceleration. (b) Chest X acceleration. (c) Pelvis X acceleration.

Fig. 5. Comparison between sled test and simulation results for the head, chest and pelvis acceleration.

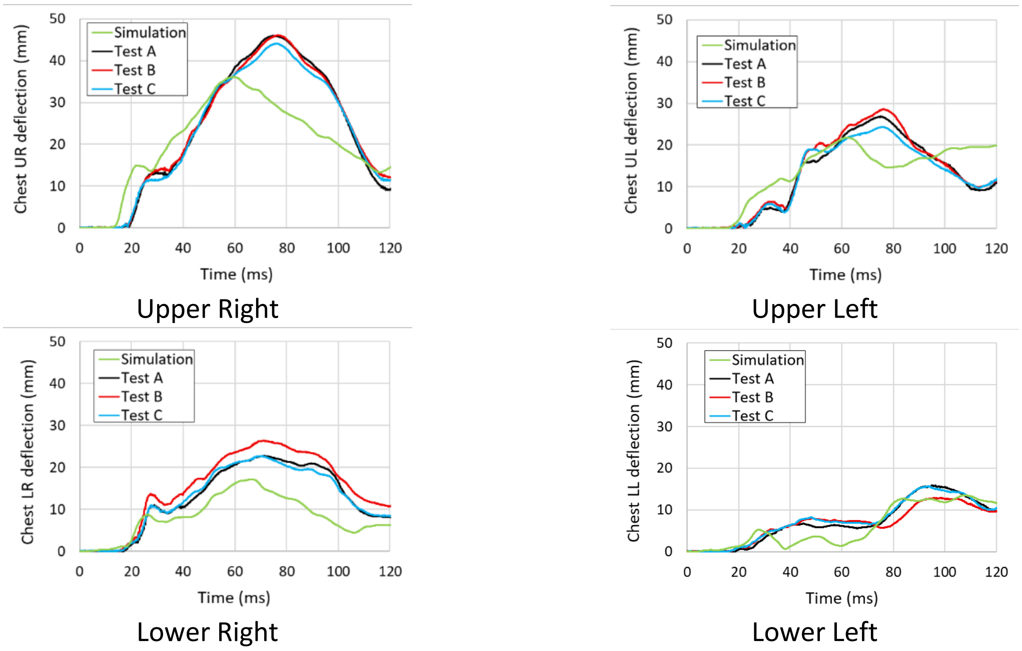

Fig. 6. Comparison between sled test and simulation results for the chest deflections.

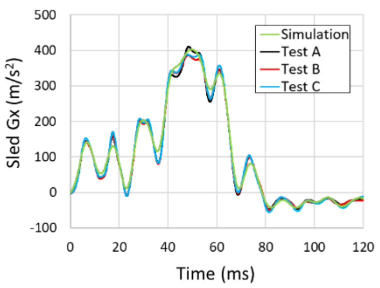

(a) Sled X acceleration.

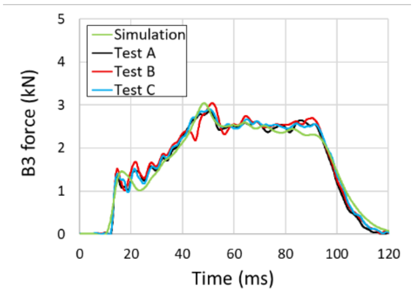

(b) Shoulder-belt force (B3).

Fig. 7. Comparison between sled test and simulation results for sled acceleration and shoulder-belt force.

TABLE III
SUMMARY OF ISO SCORE

Region	Channel	Test A	Test B	Test C	Average
Head & Neck	Head X acceleration	0.61	0.56	0.63	0.60
	Head Y acceleration	0.37	0.34	0.33	0.35
	Head Z acceleration	0.57	0.57	0.62	0.59
	Head resultant acceleration	0.62	0.58	0.63	0.61
Chest & Abdomen	Chest X acceleration	0.70	0.72	0.71	0.71
	Chest Y acceleration	0.38	0.33	0.34	0.35
	Chest Z acceleration	0.22	0.30	0.25	0.26
	Chest resultant acceleration	0.71	0.72	0.71	0.71
	Chest resultant deflection upper left	0.61	0.51	0.62	0.58
	Chest resultant deflection upper right	0.73	0.74	0.74	0.74
	Chest resultant deflection lower left	0.69	0.58	0.70	0.66
	Chest resultant deflection lower right	0.63	0.64	0.65	0.64
Knee, femur & pelvis	Pelvis X acceleration	0.84	0.85	0.84	0.84
	Pelvis Y acceleration	0.59	0.57	0.60	0.59
	Pelvis Z acceleration	0.65	0.60	0.69	0.65
	Pelvis resultant acceleration	0.84	0.83	0.84	0.84
Vehicle	Sled X acceleration	0.95	0.95	0.95	0.95
	Shoulder Belt force (B3)	0.91	0.91	0.94	0.92

TABLE IV
SUMMARY OF THORAX INJURY OUTCOMES

Injury criteria	Unit	Test			Simulation
		A	B	C	
R_{max}	mm	45.9	46.1	44.1	36.1
PC Score	-	5.1	5.3	4.9	4.1
TIC_NFR	mm	79.3	78.5	77.1	61.6

Simulation results

The global sensitivity indexes were calculated using LS-OPT (Sobol method) based on injury probabilities of simulation results. The global sensitivity indexes are summarised in Table V. The two most influential parameters for each injury criterion are highlighted in black. All thorax injury criteria were more sensitive to upper thorax stiffness than to other parameters. The second most influential parameter was changed depending on the criteria. R_{max} and *PC Score* were influenced by driver airbag pressure, and *TIC_NFR* was sensitive to load limiter force. The variation ranges and injury risk function of thorax injury criteria are shown in Fig. 8. The observed range of variation was 29–46 mm for R_{max}, 3.5–5.1 for *PC Score*, and 50–77 mm for *TIC_NFR*. The R_{max} obtained from the simulations ranged from the Euro NCAP (50 km/h) higher limit of 35 mm to the lower limit of 60 mm [1].

TABLE V
GLOBAL SENSITIVITY INDEX OF EACH PARAMETER (UNIT: %)

Parameter		R_{max}	*PC Score*	*TIC_NFR*
Dummy	Upper Thorax stiffness	**58.3**	**53.1**	**52.6**
	Lower Thorax stiffness	0.1	1.4	0.2
Boundary condition	Initial dummy posture (H-point)	3.4	0.9	15.3
	Belt routing	0.5	0.4	2.9
Restraint system	Load limiter force	9.9	15.9	**18.1**
	Driver airbag pressure (inflator property)	**27.8**	**28.2**	10.9

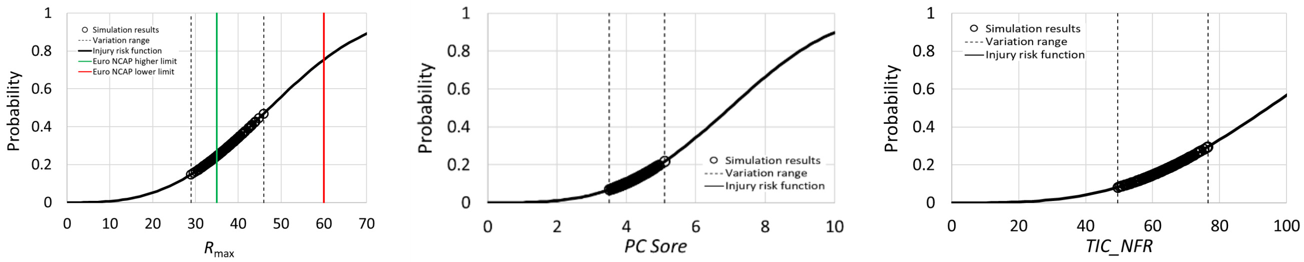

(a) R_{max}. (b) *PC Score.* (c) *TIC_NFR.*

Fig. 8. Variation range of thorax injury criteria and injury risk function.

IV. DISCUSSION

Analysis of parameter effects on R_{max}

For all thorax injury criteria, the most influential parameter was upper thorax stiffness. The occupant trajectories, upper right chest deflection, shoulder-belt (B3) force and X direction contact force between driver airbag and thorax for three cases with different upper thorax stiffness levels are shown in Fig. 9 and Fig. 10. These results correspond to the baseline upper thorax stiffness, the stiffest condition, and the softest condition, respectively, while the parameters of load limiter force and driver airbag pressure were identical. In Fig. 9, the three lines in each case represent the trajectories of the head, chest (T4), and pelvis, respectively, shown until maximum forward displacement. The occupant trajectory graphs presented in the following sections are shown in the same manner. For occupant kinematics, similar trajectories were observed in all three cases for the head, chest, and pelvis displacement. The maximum differences in forward displacement were less than 2 mm for the head, chest, and pelvis. The maximum chest deflection was measured at the upper-right position among the cases, and the chest deflection increased as upper thorax stiffness decreased. For the restraint system, the shoulder-belt loads show generally similar trends, and no clear differences are observed in the contact forces between the driver airbag and the chest in the X-direction. This indicates that the external loading to the chest is broadly similar across these cases. Therefore, the difference in chest deflection is mainly due to the variation in thorax characteristics represented by the borderline model, indicating that similar external loading can lead to different thorax deformation responses in the dummy. Considering the above discussion, it appears that variation in thorax stiffness has only a small influence on occupant kinematics but directly affects chest deflection.

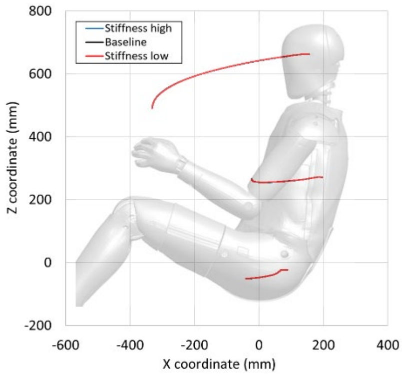

Fig. 9. Occupant trajectory (different upper thorax stiffness).

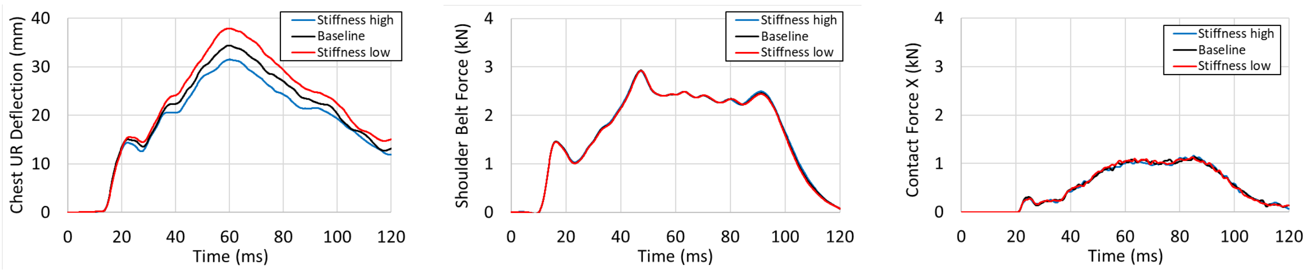

(a) Chest deflection. (b) Shoulder-belt force (B3). (c) Driver airbag contact force.

Fig. 10. Time history of chest deflection, shoulder-belt force and X direction contact force between driver airbag and thorax (different upper thorax stiffness).

R_{max} also showed high sensitivity to variation in driver airbag pressure. Figures 11–12 show the occupant kinematics, upper-right chest deflection, shoulder-belt force and X direction contact force between driver airbag and thorax for three cases with different driver airbag pressure levels. These results correspond to the baseline driver airbag pressure, the highest pressure, and the lowest pressure, respectively, while the parameters of upper thorax stiffness, dummy initial posture, shoulder-belt routing, and load limiter force were identical. For occupant kinematics, the head and chest forward displacements increased as driver airbag pressure decreased. The forward displacement of pelvis was nearly the same among three cases. The maximum differences in forward displacement among the cases were approximately 78 mm for the head, 26 mm for the chest, and 2 mm for the pelvis. The maximum chest deflections were observed at the upper-right measurement point, and deflection increased as driver airbag pressure increased. As shown in Fig. 12(c), the maximum contact force of driver airbag varied by 0.5 kN among the three cases. On the other hand, no clear differences were observed in the loading from the shoulder-belt. These findings suggest that loading from driver airbag contributed to the increase in R_{max}, leading to its high sensitivity.

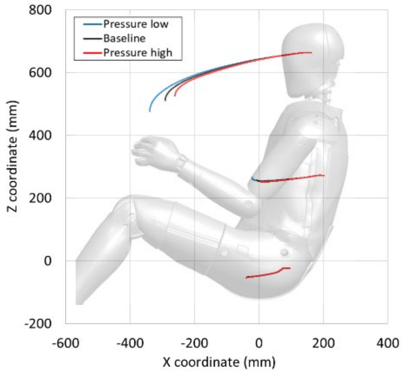

Fig. 11. Occupant trajectory (different driver airbag pressure level).

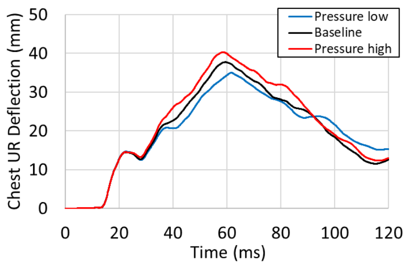

(a) Upper-right chest deflection.

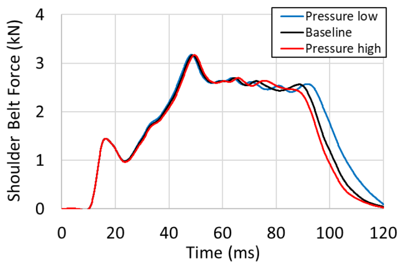

(b) Shoulder-belt force (B3).

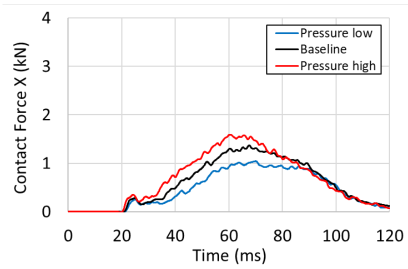

(c) Driver airbag contact force.

Fig. 12. Time history of chest deflection, shoulder-belt force and X direction contact force between driver airbag and thorax (different driver airbag pressure level).

Analysis of parameter effects on PC Score

Regarding the *PC Score*, the parameter with the highest sensitivity was the upper thorax stiffness, and the second most sensitive parameter was the driver airbag pressure (Table V). The *PC Score* is defined using the upper and lower maximum thorax deflections as well as left–right differences in the upper and lower deflections. Figure 13 shows the breakdown of each term within *PC Score* from simulation results shown in Figs 9–12. For the influence of upper thorax stiffness, the component of upper total deflection was the largest proportion (approximately 40%) among the components of the *PC Score.* The upper total deflection is calculated from the sum of maximum left and right upper thorax deflections. As observed in the analysis of R_{max}, the upper deflection was affected by the upper thorax stiffness, therefore *PC Score* was considered to be sensitive to the upper thorax stiffness. In addition, no clear differences were observed for the other components of *PC Score*. Regarding the effect of driver airbag pressure, differences in the upper total deflection component were observed among the cases. As discussed above, loading on the chest increased as driver airbag pressure increased. Since the driver airbag contacted mainly with the upper thorax, differences in the lower total deflection component were smaller than that of upper total deflection component. The upper total deflection component was the largest component of the *PC Score*, therefore the sensitivity of driver airbag pressure scored relatively high on the *PC Score*. Under the conditions of this study, the driver airbag contacted the occupant almost symmetrically (Fig. 14). Hence, the components, including left-right deflection differences, did not show clear variations. It should be noted that only the X-axis acceleration was applied in the sled simulations. Therefore, lateral movement of the vehicle was not considered in this study.

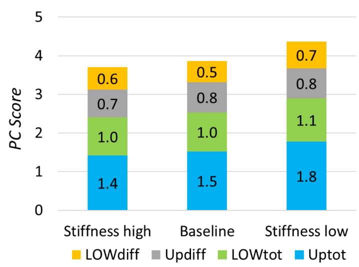

(a) Upper thorax stiffness.

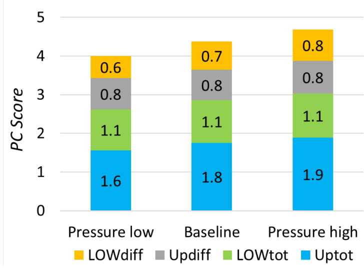

(b) Driver airbag pressure.

Fig. 13. Breakdown of the *PC Score* components.

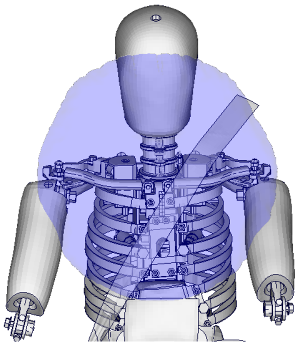

Fig. 14. Front view of the contact between the dummy and the driver airbag. The blue surface shows the area where the airbag is in contact with the chest. The figure shows the simulation result under the baseline conditions at the timing of maximum upper-right chest deflection.

Analysis of parameter effects on TIC_NFR

Regarding the *TIC_NFR*, the parameter with the highest sensitivity was the upper thorax stiffness, and the second most sensitive parameter was the load limiter force (Table V). The *TIC_NFR* is calculated using R_{max} and the upper deflection difference. Figure 15 shows the breakdown of each component within *TIC_NFR* from simulation results shown in Fig. 9 and Fig. 10. The results shown in Fig. 15(b) correspond to the baseline load limiter force, the highest force, and the lowest force, respectively, while the parameters of upper/lower thorax stiffness, initial dummy posture, and driver airbag pressure were identical. R_{max} is directly included in the calculation and accounts for approximately 60% of the *TIC_NFR*. Thus, similar to R_{max}, upper thorax stiffness is considered to have a higher influence on *TIC_NFR*. The differences observed in the upper deflection difference component were relatively small compared with the R_{max} component because, in this study, the upper thorax stiffness was adjusted without changing the left-right stiffness distribution. For the influence of load limiter force, both the R_{max} and upper deflection difference components increased as load limiter force increased. The shoulder-belt was routed over the upper-right deflection sensor (Fig. 4(a)), resulting in the upper-right chest deflection tending to increase more with higher shoulder-belt forces. Thus, the upper deflection differences were increased as load limiter force increased.

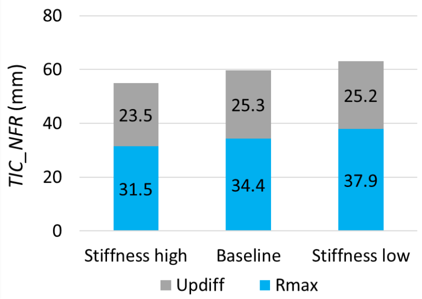

(a) Upper thorax stiffness.

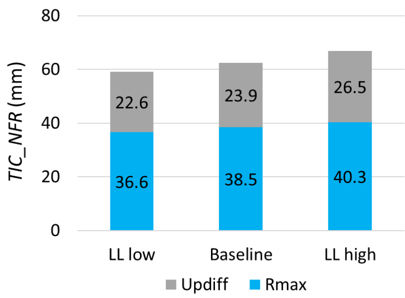

(b) Load limiter force.

Fig. 15. Breakdown of the *TIC_NFR* components.

Influence on Current Assessment Results

The variation range of the R_{max} was 17 mm (29–46 mm), which is within the broader range of variation reported in previous physical test and simulation studies [4-5][10] (Appendix Table D1). In addition, the highest R_{max} exceeded the upper limit of Euro NCAP rating scheme (35 mm), and the repeated physical test results (Table IV) also exceeded this limit. This indicates that both physical test variation and simulation-based variation can cause the R_{max} value to exceed the upper limit. In the colour-band scheme introduced by Euro NCAP from 2026 [1], the width of the R_{max} colour band is 8.3 mm, and the variation range observed in the simulation results was greater than this width (Fig. 16). This result indicates that it may lead to a change of up to two levels in the score (colour) for the load case considered in this study. A previous study showed that updating the dummy certification corridor for the upper thorax could be one option to limit the influence of variation in thorax characteristics on chest deflection response [10]. However, if the certification corridor is narrowed without a sufficient understanding of the root causes of the variation, this may increase the number of certification tests and the frequency of dummy parts replacement. The results observed in this study reflect variation in thorax characteristics represented in the dummy model, whereas the root causes of such variation in real-world testing were not directly identified in this study. Previous studies have reported possible contributors such as rib thickness and rib temperature [21-22], but further investigation is needed to clarify the causes of this variation. These findings suggest that minimising the influence of THOR-50M upper thorax variation would help to reduce the variation of the rating results. Injury criteria should remain sensitive to restraint system characteristics, but further efforts should be made to establish robust criteria that are not overly influenced by variations in test conditions. Additionally, enhancing the scoring method in assessment testing could also be effective in limiting the effects of testing variabilities.

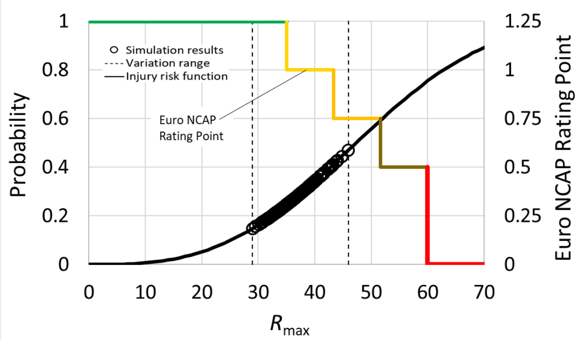

Fig. 16. Occupant trajectory (comparison of upper thorax stiffness).

Limitation

Since the sled simulations were performed using the sled pulse applied only in an X-axis, potential effects of vehicle oblique or pitch motions were not captured in this investigation. In addition, the simulations were conducted using a single small SUV vehicle environment. Therefore, the sensitivity rankings identified in this study may not be directly transferable to all vehicle segments. Some assumed parameter ranges, including those for belt routing and the restraint system, were not derived from quantitative measurements but from practical estimates based on expert input and testing experience. Although the variation ranges for each parameter were assumed to reflect conditions that may occur in physical testing, these ranges may change depending on the vehicle and the specific test configuration. In addition, possible interaction effects between parameters (e.g. dummy initial posture and seatbelt routing) were not investigated in this study. For the simulation model used in this study, differences in the peak value and timing of chest deflection were observed, and the results of *PC Score* and *TIC_NFR* were affected by left-right and upper-lower deflection differences. Further investigation is needed to confirm whether the sensitivities observed in the DOE simulations can also be observed in physical tests.

V. CONCLUSION

This investigation showed that the sensitivity of THOR-50M to upper thorax stiffness was higher than to test boundary conditions or restraint system properties. The maximum variation in chest deflection (R_{max}) observed in the DOE simulations exceeded the Euro NCAP rating higher limit, and the variation range was greater than the colour band width. These findings indicate that the results of current thorax rating may be influenced by parameter variation considered in this study. Therefore, it is important to minimise the influence of THOR-50M upper thorax stiffness variation in physical testing when evaluating the performance of safety systems and assessment programs. Enhancing the scoring method in the assessment programs could be effective for limiting the variability effects. While injury criteria should remain sensitive to restraint system properties, considering the injury criteria that are less sensitive to testing variations could be an effective way to limit the influence of physical testing variability. The injury criteria are intended to represent human response sensitivity to different safety systems, without showing excessive sensitivity to variations in test conditions. Further investigation into the robustness of thorax injury criteria is necessary as future research.

VI. ACKNOWLEDGEMENTS

Generative artificial intelligence tools (ChatGPT, OpenAI) were used to support language editing. All scientific

content, interpretations, and conclusions were developed, reviewed, and validated by the authors, who take full responsibility for the accuracy and integrity of the work.

VII. REFERENCES

[1] Euro NCAP (2025) Crash Protection Frontal Impact Protocol Version 1.1, September 2025, Brussels.

[2] National Highway Traffic Safety Administration (NHTSA) (2023) Notice of Proposed Rulemaking (NPRM): Anthropomorphic Test Devices; THOR 50th Percentile Adult Male Test Dummy, Federal Register, Vol. 88, No. 172, September 7, 2023, Washington, D.C., USA.

[3] Euro NCAP (2025) THOR 50th Specification and Certification Technical Bulletin CP 106 Version 2.1, July 2025, Brussels.

[4] Gehre, C. (2019) THOR 50-M R&R compared to current consumer rating schemes, ISO/TC22/SC36/WG5/N1210, November 2019.

[5] Wernicke, P. (2024) R&R of THOR Chest Response in Vehicle Environment: A Unique Data Set for Worldwide Collaboration. *Proceedings of the AIRBAG 2024 Conference*, Mannheim, Germany.

[6] Hohage, B., Mittermeier, F., Gehre, C., Meier, A. (2017) Differences of the Chest Deflection Between Different THOR Specimens, ISO/TC22/SC36/WG5/N1171, 2017.

[7] Hikida, K., Maehara, K., Mikami, H., Mae, H. (2017) Repeatability and Reproducibility of Upper Thorax Responses of THOR-50M ATDs. *Proceedings of the 25th Enhanced Safety of Vehicles (ESV) Conference, Detroit, Michigan, USA*.

[8] Kronwitter, S., Rajyaguru, P., Segura, R., Birkefeld, K., Kösters, M. (2024) Accounting for and Dealing with Uncertainty Inherent to ATDs in the Design of Occupant Safety Systems. *Proceedings of the Airbag 2024 Conference*, Mannheim, Germany.

[9] Eggers, A., Eickhoff, B., Dobberstein, J., Zellmer, H., Adolph, T. (2014) Effects of Variations in Belt Geometry, Double Pretensioning and Adaptive Load Limiting on Advanced Chest Measurements of THOR and Hybrid III. *Proceedings of the IRCOBI Conference*, 2014, Berlin, Germany.

[10] Furukawa, D. and Eggers, A. (2026) Sensitivity of THOR-50M injury outcomes to assessment testing variability in frontal crash. *Proceedings of the 28th Enhanced Safety of Vehicles (ESV) Conference, Toronto, Canada*

[11] Euro NCAP (2025) Data Acquisition and Injury Calculation: Crash Protection, Technical Bulletin CP-005, Version 1.3, Brussels.

[12] Humanetics Innovative Solutions, Inc. (2021) THOR-50M Euro NCAP LS-DYNA Borderline FE Model, Release Version V1.8, Technical Report and User's Manual.

[13] Livermore Software Technology Corporation (2018) LS-DYNA Keyword User's Manual Version R11, LSTC, California.

[14] Euro NCAP (2023) THOR Specification and Certification Technical Bulletin TB026 Version 1.3, February 2023, Brussels.

[15] Stander, N., Basudhar, A., *et al*. (2019) LS-OPT User's Manual: A Design Optimization and Probabilistic Analysis Tool for the engineering analyst Version 6.0. 2019.

[16] Craig, M., Parent, D., *et al.* (2020) Injury Criteria for the THOR 50th Male ATD, September 2020.

[17] Poplin, G. S., McMurry, T. L., *et al.* (2017) Development of Thoracic Injury Risk Functions for the THOR ATD. *Accident Analysis & Prevention*, **106**: pp. 122–130.

[18] Xavier, T. and Pascal, B. (2019) Updated Chest Injury Criterion for the THOR Dummy. *Proceedings of the 26th ESV Conference*, 2019, Eindhoven, The Netherlands.

[19] International Organization for Standardization (ISO) (2021) ISO/TR 19222: Road vehicles — Injury risk curves for the THOR dummy.

[20] Euro NCAP (2025) Crash Protection: Virtual Testing Protocol, Version 1.0.2, Brussels.

[21] Masuda, M., Yaguchi, M., *et al*. (2021) Development of Rib Drop Test Method for THOR 50M, *Proceedings of the Society of Automotive Engineers of Japan (JSAE) Autumn Conference*.

[22] Hartlieb, M., Lasslop, Y., (2016) THOR-Dummy Temperature Study, ISO/TC22/SC36/WG5/N1124, 2016.

VIII. APPENDIX

A. Comparison of initial dummy posture between the physical sled test and the simulation model

Tables A1–A2 show comparisons of the initial dummy posture coordinates in the X- and Z-directions and the tilt sensor angles between the physical tests and the simulation model. Each coordinate is given relative to the H-point, and the coordinate system is defined as shown in Fig. 9. Figure A1 illustrates the belt routing parameter described in the manuscript, defined as the relative vertical distance between the lower neck bolt and the upper edge of the shoulder-belt. Figure A2 shows the comparison of the initial belt routing. The belt routing parameter in the simulation model was set to 69 mm based on the physical test measurements.

TABLE A1

COMPARISON OF INITIAL DUMMY POSTURE COORDINATES IN THE X- AND Z- DIRECTION

		Test						Simulation	
		A		B		C			
		X	Z	X	Z	X	Z	X	Z
Head CoG		160	650	160	649	160	650	160	659
Shoulder	Left	149	404	146	401	148	402	122	414
	Right	147	399	148	399	147	402	122	414
Knee	Left	-395	130	-399	130	-396	130	-393	139
	Right	-395	136	-398	136	-397	134	-395	145
Heel	Left	-669	-296	-669	-296	-671	-298	-668	-288
	Right	-663	-287	-662	-286	-665	-288	-662	-289

Unit: mm

TABLE A2

COMPARISON OF INITIAL DUMMY POSTURE ANGLE (TILT SENSOR VALUE)

	Test			Simulation
	A	B	C	
Head	-9.3	-9.0	-9.1	-9.3
Neck/T1	-6.0	-6.0	-6.2	-6.0
T6	17.8	18.6	18.2	17.8
T12	27.0	27.8	27.5	27.0
Pelvis	33.1	32.9	33.0	33.1

Unit: degree

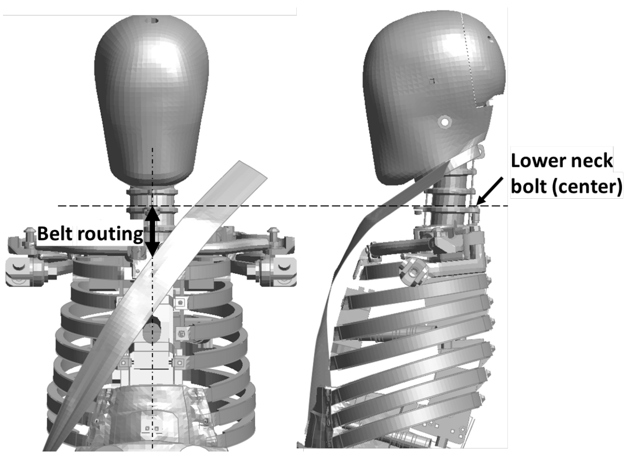

Fig. A1. Definition of the seat belt routing parameter.

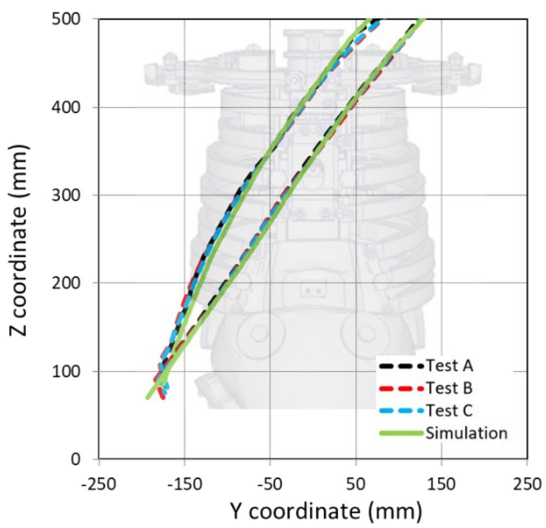

Fig. A2. Comparison of initial seatbelt routing.

B. Repeatability in the repeated baseline sled tests

Table B1 shows a summary of the repeatability of these baseline sled tests for the major response channel.

TABLE B1

SUMMARY OF REPEATABILITY IN THE REPEATED BASELINE SLED TESTS FOR THE MAJOR RESPONSE CHANNEL

Metrics			Unit	Test		
				A	B	C
Sled acceleration	OLC		g	24.8	24.5	25.0
Chest deflection	Maximum resultant deflection	Upper Left	mm	26.9	28.6	24.4
		Upper Right	mm	45.9	46.1	44.1
		Lower Left	mm	15.9	12.9	15.7
		Lower Right	mm	22.8	26.4	22.8
	Peak timing	Upper Left	ms	75.2	76.2	75.8
		Upper Right	ms	74.5	76.6	76.2
		Lower Left	ms	95.3	99	93.3
		Lower Right	ms	71.3	71.4	70.4
Belt force	Maximum force	Shoulder-belt (B3)	kN	2.9	3.0	2.9

C. Statistics of the simulation outcomes for the thorax injury criteria

Table C1–C2 summarise the minimum, maximum, mean, and standard deviation of the thorax injury outcomes from the simulation results, including the injury values and injury probabilities.

TABLE C1

SUMMARY STATISTICS OF THE SIMULATION OUTCOMES FOR THE THORAX INJURY CRITERIA (INJURY VALUES)

	R_{max} (mm)	*PC Score* (-)	*TIC_NFR* (mm)
Minimum	29.0	3.5	49.6
Maximum	45.9	5.1	76.6
Mean	36.9	4.2	63.0
Standard Deviation	3.5	0.3	6.0

TABLE C2

SUMMARY STATISTICS OF THE SIMULATION OUTCOMES FOR THE THORAX INJURY CRITERIA (INJURY PROBABILITIES, UNIT: %)

	R_{max}	*PC Score*	*TIC_NFR*
Minimum	14.8	6.9	8.2
Maximum	46.9	21.8	29.6
Mean	28.5	12.4	17.3
Standard Deviation	6.7	3.0	4.8

D. Comparison of chest deflection variation ranges between this study and previous studies

Table C2 compares the maximum chest deflection (R_{max}) variation ranges reported in this study with those reported in previous studies.

TABLE D1

COMPARISON OF CHEST DEFLECTION VARIATION RANGES BETWEEN THIS STUDY AND PREVIOUS STUDIES

Study	Method	Environment	Variation reported	Remarks
This study	Simulation (DOE)	Production vehicle	29–46 mm (Range: 17 mm)	–
[4]	Repeated sled test	Generic	36–45 mm (Range: 9 mm)	Includes multiple dummy manufacturers
[5]	Physical test (test configuration not clearly specified)	Production vehicle	Range: approximately 16 mm (exact value not reported)	Includes multiple dummies
[5]	Repeated sled test	Production vehicle	Range: 9.3 mm	Includes multiple dummies
[5]	Repeated sled test	Production vehicle	Range: 8.4 mm	Includes multiple dummies
[10]	Simulation (DOE)	Generic	28–41 mm (Range: 13 mm)	Includes variation in thorax characteristics